Report

Cell Reports

Mitochondrial Protein Synthesis and mtDNA Levels Coordinated through an Aminoacyl-tRNA Synthetase Subunit

Graphical Abstract

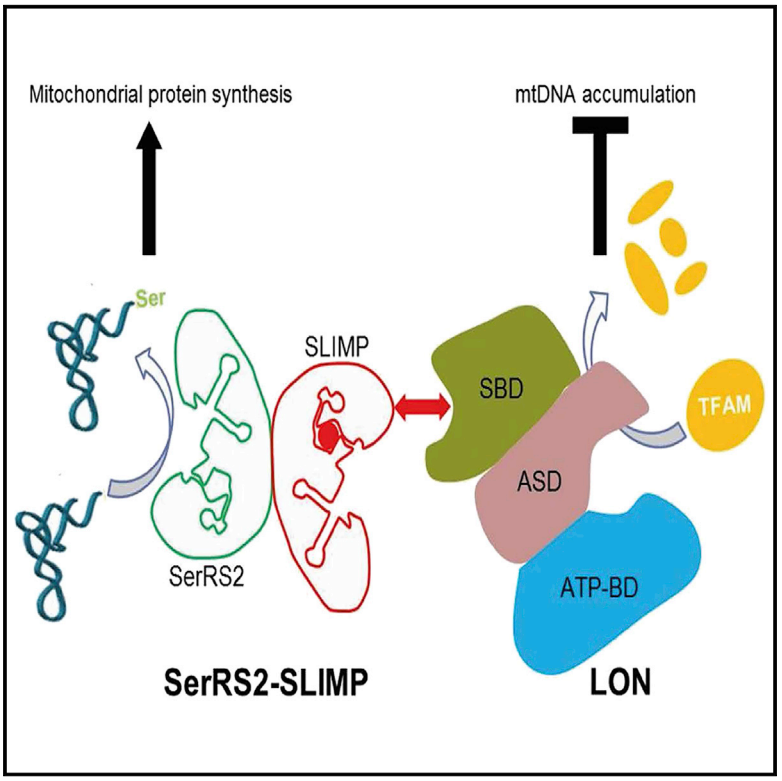

Highlights

- *Drosophila* SerRS2 is a heterodimer formed by SerRS2 and SLIMP monomers
- SLIMP is essential for tRNA-Ser aminoacylation
- SLIMP interacts with LON protease to stimulate TFAM degradation
- SLIMP depletion induces a cell-cycle arrest in G2 phase

Authors

Daria Picchioni, Albert Antolin-Fontes, Noelia Camacho, ..., Laurie S. Kaguni, Travis H. Stracker, Lluís Ribas de Pouplana

Correspondence

lluis.ribas@irbbarcelona.org

In Brief

Picchioni et al. report the architecture of a housekeeping enzyme that is essential for mitochondrial protein synthesis. This enzyme is a heterodimer that contains a catalytically active subunit and an inactive but essential monomer (SLIMP). SLIMP also interacts with a major mitochondrial protease to control mitochondrial DNA levels.

Picchioni et al., 2019, Cell Reports *27*, 40–47
April 2, 2019
https://doi.org/10.1016/j.celrep.2019.03.022

CellPress

OPEN ACCESS
CellPress

Cell Reports
Report

Mitochondrial Protein Synthesis and mtDNA Levels Coordinated through an Aminoacyl-tRNA Synthetase Subunit

Daria Picchioni,[1,9] Albert Antolin-Fontes,[1,9] Noelia Camacho,[1] Claus Schmitz,[2] Alba Pons-Pons,[1] Marta Rodríguez-Escribà,[1] Antigoni Machallekidou,[1] Merve Nur Güler,[1] Panagiota Siatra,[1] Maria Carretero-Junquera,[1] Alba Serrano,[1] Stacy L. Hovde,[3] Philip A. Knobel,[1,4] Eva M. Novoa,[5,6] Maria Solà-Vilarrubias,[2] Laurie S. Kaguni,[3,7] Travis H. Stracker,[1] and Lluís Ribas de Pouplana[1,8,10,*]

[1]Institute for Research in Biomedicine (IRB Barcelona), the Barcelona Institute of Science and Technology, Parc Científic de Barcelona, C/Baldiri Reixac 10, 08028 Barcelona, Catalonia, Spain
[2]Structural MitoLab, Department of Structural Biology, Molecular Biology Institute Barcelona (IBMB-CSIC), Barcelona, Spain
[3]Department of Biochemistry and Molecular Biology and Center for Mitochondrial Science and Medicine, Michigan State University, East Lansing, MI, USA
[4]Laboratory for Molecular Radiobiology, Clinic of Radiation Oncology, University of Zurich, 8057 Zurich, Switzerland
[5]Centre for Genomic Regulation (CRG), the Barcelona Institute of Science and Technology (BIST), Doctor Aiguader 88, 08003 Barcelona, Spain
[6]Garvan Institute of Medical Research, 384 Victoria Street, 2010 Darlinghurst, NSW, Australia
[7]Institute of Biosciences and Medical Technology, University of Tampere, 33014 Tampere, Finland
[8]Catalan Institution for Research and Advanced Studies (ICREA), P/Lluis Companys 23, 08010 Barcelona, Catalonia, Spain
[9]These authors contributed equally
[10]Lead Contact
*Correspondence: lluis.ribas@irbbarcelona.org
https://doi.org/10.1016/j.celrep.2019.03.022

SUMMARY

The aminoacylation of tRNAs by aminoacyl-tRNA synthetases (ARSs) is a central reaction in biology. Multiple regulatory pathways use the aminoacylation status of cytosolic tRNAs to monitor and regulate metabolism. The existence of equivalent regulatory networks within the mitochondria is unknown. Here, we describe a functional network that couples protein synthesis to DNA replication in animal mitochondria. We show that a duplication of the gene coding for mitochondrial seryl-tRNA synthetase (SerRS2) generated in arthropods a paralog protein (SLIMP) that forms a heterodimeric complex with a SerRS2 monomer. This seryl-tRNA synthetase variant is essential for protein synthesis and mitochondrial respiration. In addition, SLIMP interacts with the substrate binding domain of the mitochondrial protease LON, thus stimulating proteolysis of the DNA-binding protein TFAM and preventing mitochondrial DNA (mtDNA) accumulation. Thus, mitochondrial translation is directly coupled to mtDNA levels by a network based upon a profound structural modification of an animal ARS.

INTRODUCTION

Aminoacyl-tRNA synthetases (ARSs) are essential enzymes whose canonical function is the aminoacylation of tRNAs with their cognate amino acid (Ibba and Soll, 2000). In addition, ARSs represent evolutionary hot points that readily incorporate new domains to acquire non-canonical regulatory functions (Guo and Schimmel, 2013; Yao et al., 2014; Dong et al., 2000; Efeyan et al., 2015; González and Hall, 2017; Arif et al., 2017). Mammalian cytosolic seryl-tRNA synthetases (SerRSs) have been identified as essential regulators of cardiovascular development (Amsterdam et al., 2004; Fukui et al., 2009; Herzog et al., 2009).

SerRSs are homodimeric enzymes that belong to the subclass IIa of ARS (Eriani et al., 1990; Ribas de Pouplana and Schimmel, 2001) and are in charge of the serylation of $tRNA^{Ser}$. The structure of the SerRS monomer comprises an active site domain and an N-terminal domain that folds into a long coiled-coil structure (Cusack et al., 1990) that recognizes the variable arm of $tRNA^{Ser}$. In metazoans, SerRS are among the few duplicated ARS; one isoform acts in the cytosol and a second acts in the mitochondria. The three-dimensional structures of mitochondrial and cytosolic SerRSs are fundamentally similar (Chimnaronk et al., 2005).

During the investigation of the function of *Drosophila* mitochondrial SerRS (DmSerRS2) (Guitart et al., 2010, 2013), we discovered SLIMP (*CG31133*; BcDNA: LD24627), a paralog of DmSerRS2 present in arthropods and echinoderms that retains a typical mitochondrial SerRS structure but has lost all tRNA aminoacylation activity (Guitart et al., 2010). We have reported that SLIMP depletion *in vivo* severely affects mitochondrial function, increases mtDNA levels, and is lethal at any stage of development (Guitart et al., 2010).

To investigate the biological function of SLIMP, we have characterized its protein interactome and found that SLIMP interacts

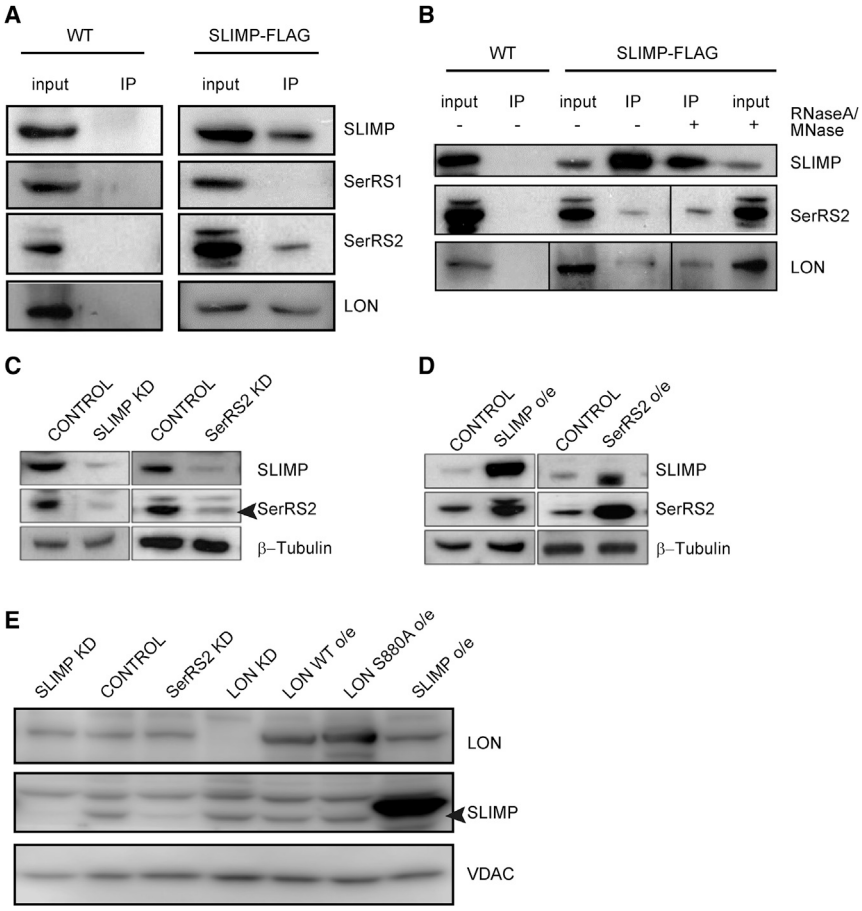

Figure 1. SLIMP Interacts with DmSerRS2 and LON Protease

(A) Immunoblot analyses of control (wild-type [WT]) and SLIMP-FLAG immunoprecipitated (IP) samples.

(B) Immunoblot of IP samples treated with RNaseA/micrococcal nuclease (MNase) treatment.

(C and D) Immunoblot of (C) SLIMP-depleted and DmSerRS2-depleted cells or (D) cells overexpressing SLIMP or DmSerRS2 cells compared to control cells.

(E) Immunoblot analysis of LON and SLIMP in control cells, cells depleted for SLIMP, DmSerRS2, and LON, and cells overexpressing LON, LON S880A, and SLIMP. Voltage-dependent anion channel (VDAC) protein levels are used as a loading control.

See also Figure S1.

with DmSerRS2 and with the mitochondrial protease LON. LON protease is an essential mitochondrial protein (Pinti et al., 2015, 2016) belonging to the family of ATP-dependent serine proteases whose structure includes three distinct domains: an ATP-binding domain, a substrate-binding domain, and a catalytic domain (Park et al., 2006; Stahlberg et al., 1999). LON contributes to mitochondrial protein quality control by degrading misfolded proteins to prevent their aggregation (Bezawork-Geleta et al., 2015; Bota and Davies, 2002). LON is also a component of mitochondrial nucleoids, where it degrades mitochondrial transcription factor A (TFAM) (Alam et al., 2003; Bogenhagen, 2012). TFAM is a major nucleoid component that binds to mtDNA and regulates mtDNA copy number (Gangelhoff et al., 2009). In *Drosophila*, LON regulates mtDNA copy number and transcription by selective degradation of TFAM (Matsushima et al., 2010).

Here, we show that the SLIMP-DmSerRS2 interaction results in a stable heterodimer that is essential for tRNA aminoacylation, protein synthesis, and mitochondrial respiration. As expected from its involvement in protein synthesis, we found that SLIMP localizes in the mitochondrial matrix in close proximity to ribosome granules. In addition, SLIMP participates in the regulation of mtDNA copy number by stimulating the degradation of TFAM by LON through an interaction with the substrate-binding domain of this protease.

Two independent genetic screens in *Drosophila* identified SLIMP as an important factor for cell-cycle progression (Ambrus et al., 2009; Liang et al., 2014). SLIMP depletion was found to compensate for *Drosophila* E2F (dE2F) pathway inactivation, allowing cell-cycle progression from G1 to S phase in the absence of dE2F1 through a mechanism that is independent of the retinoblastoma-E2F (RB-E2F) pathway (Ambrus et al., 2009). In agreement with these reports, we show here that depletion of SLIMP but not of SerRS2 or LON induces a cell-cycle arrest in G2. This effect can be rescued by overexpressing SLIMP, but not SerRS2 or LON. Thus, *Drosophila* SerRS2 has evolved an idiosyncratic structure that coordinates protein synthesis to mtDNA levels and plays a role in cell-cycle control.

RESULTS

SLIMP Interacts with DmSerRS2 and LON Protease

To investigate the biological function of SLIMP, we characterized its protein interactome by pull-down assays using SLIMP fused to a tandem affinity purification tag (SLIMP-TAP) (Figure S1A; Table S1). Initial hits were confirmed by co-immunoprecipitation (coIP) with an α-FLAG antibody. These experiments independently showed that SLIMP interacts with both DmSerRS2 and the mitochondrial protease LON (Figure 1A). Nuclease treatments did not affect the interactions, indicating that SLIMP binds to DmSerRS2 and LON independently of nucleic acids (Figure 1B).

The interdependence between SLIMP, DmSerRS2, and LON levels was examined by monitoring RNA and protein levels after RNAi knockdown of each gene. Depletion of either SLIMP or DmSerRS2 did not change the transcript levels of the other gene (Figure 1C); however, their protein levels were interdependent, indicating that the SLIMP-DmSerRS2 interaction confers stability to both proteins (Figures 1D and S1B–S1E). SLIMP

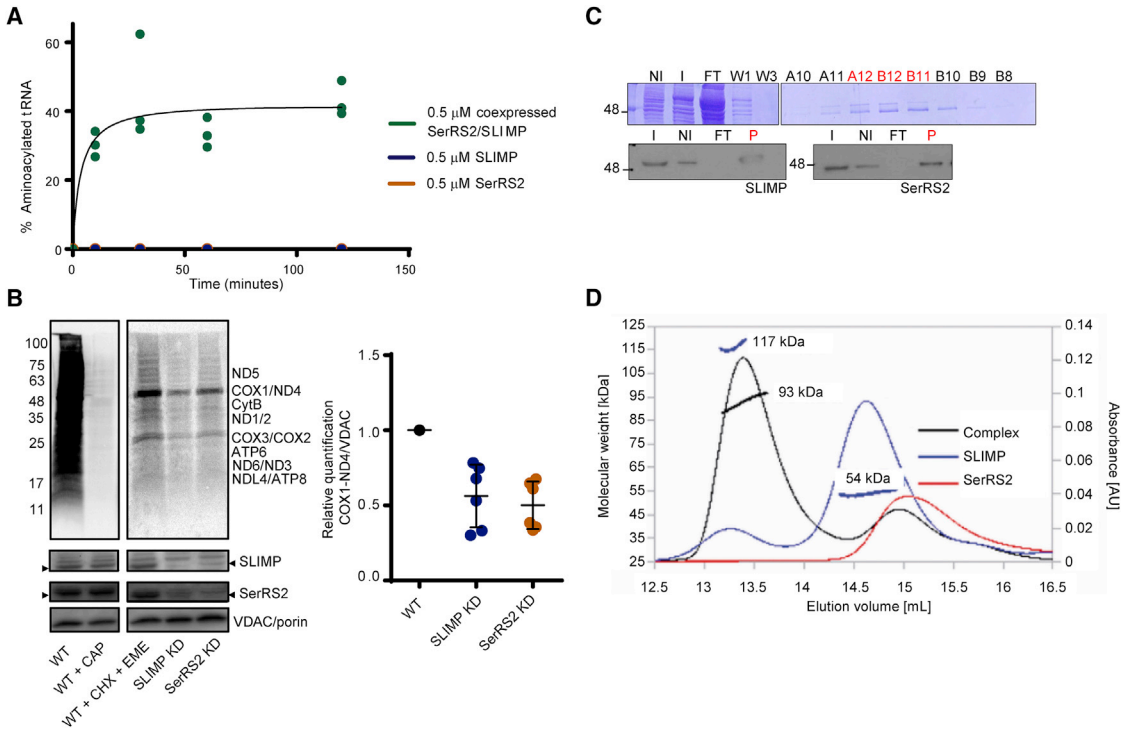

Figure 2. SLIMP Activates DmSerRS2 and Is Required for Mitochondrial Translation

(A) mt-tRNA$^{Ser}_{GCU}$ aminoacylation assays. The activity percentage of the purified SLIMP-DmSerRS2 complex is shown in green. Data represent means ± SEMs of three independent experiments.

(B) Phosphorimager images of S35 labeled mitochondrial translation products separated by SDS-PAGE and blotted to polyvinylidene fluoride (PVDF) membranes are shown for the indicated cell lines. Untreated control cells (WT) and cells treated with chloramphenicol (WT + CAP) were evaluated. SLIMP-depleted, DmSerRS2-depleted, and control cells were treated with cycloheximide and emetine (WT + CHX + EME) to analyze mitochondrial translation. SLIMP and DmSerRS2 protein levels were analyzed by immunoblot, and the VDAC protein level was analyzed to ensure equal loading. Quantification of individual values from two independent experiments performed in triplicate is shown.

(C) Co-expression and purification of ΔN-SLIMP and ΔN-DmSerRS2 in *E. coli*. SDS-PAGE analysis of not-induced bacteria (NI), induced (I), flow through (FT), washes (W1 and W3), and elution fractions (A10–B8). Immunoblot against His-tagged (DmSerRS2) and Strep-tagged (SLIMP) from I, NI, FT, and P (A12, B12, and B11 fractions).

(D) Estimation of the absolute molecular weight of the DmSerRS2/SLIMP complex and the free proteins by flow-mode multiangle laser light scattering (MALLS). UV traces from the DmSerRS2/SLIMP complex (black), free DmSerRS2 (red) and free SLIMP (blue), after size exclusion chromatography (SEC). The absolute molecular weight (MW) obtained by MALLS is represented for each peak, except for DmSerRS2, the instability of which precluded a consistent MW estimation. See also Figure S2.

and LON levels were independent, indicating that their interaction does not stabilize the proteins and that SLIMP is not degraded by LON (Figures 1E, S1F, and S1G).

SLIMP and DmSerRS2 Form a Heterodimer Required for Mitochondrial Translation

Having previously shown that SLIMP is catalytically inactive, we tested whether the SLIMP-DmSerRS2 interaction influenced the enzymatic activity of DmSerRS2. Aminoacylation assays with purified SLIMP, DmSerRS2, and both proteins simultaneously showed that only the co-purified DmSerRS2-SLIMP complex could efficiently aminoacylate mitochondrial tRNA$^{Ser}_{(GCU)}$ and tRNA$^{Ser}_{(UGA)}$ (Figure 2A). We titrated increasing concentrations of SLIMP to a fixed concentration of DmSerRS2 (Figure S2A) and measured aminoacylation activity at different tRNA$^{Ser}_{(GCU)}$ concentrations (Figures S2B and S2C). This showed that the requirement for SLIMP is independent of substrate concentration and that activation of DmSerRS2 by SLIMP is dose dependent.

We tested the impact of adding SLIMP to aminoacylation reactions performed by other SerRSs. SLIMP did not activate the aminoacylation of tRNA^{Ser} substrates by eukaryotic, cytosolic, or bacterial SerRSs. However, SLIMP did stimulate the aminoacylation of both *Strongylocentrotus droebachiensis* (sea urchin) tRNA$^{Ser}_{(GCU)}$ and *Streptococcus pneumoniae* tRNA$^{Ser}_{(GCU)}$ by DmSerRS2, demonstrating that SLIMP activation is specific for DmSerRS2 and independent of tRNA substrate (Tables S2 and S3; Figure S2H).

We then performed a pulse-labeling assay to determine whether the rate of mitochondrial translation in S2 cells was influenced by the depletion of DmSerRS2 or SLIMP. Following the depletion of either SLIMP or DmSerRS2, we detected a comparable decrease in mitochondrial translation in both cases (Figure 2B). As expected, this decrease in translational activity is

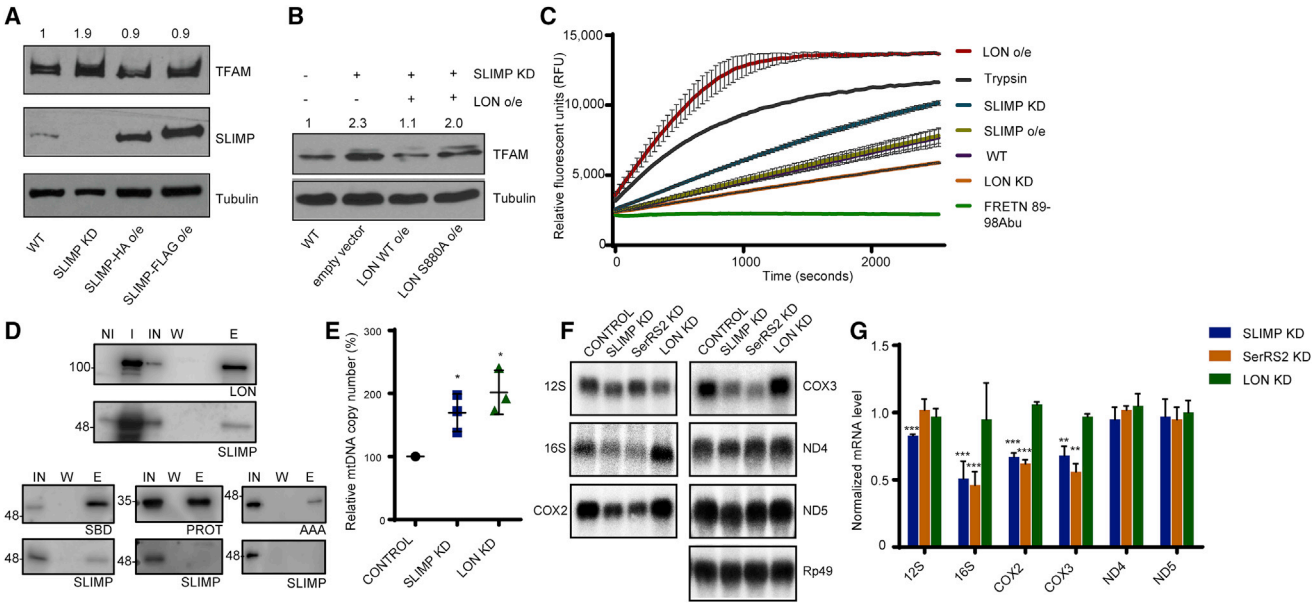

Figure 3. SLIMP Activates the Specific Degradation of TFAM by LON Protease

(A) Immunoblot analyses of TFAM and SLIMP, upon SLIMP knockdown or overexpression. Band quantification is normalized to S2 WT cells.

(B) Immunoblot analyses of TFAM levels upon SLIMP knockdown and with or without LON overexpression (LON WT or the mutated form LON S880A).

(C) LON protease activity assay using FRETN 89–98Abu and monitoring the relative fluorescence during time (s). The means of three independent experiments ± SDs are shown.

(D) Co-expression and purification of ΔN-SLIMP and ΔN-LON or each subdomain substrate-binding domain (SBD), proteolytic domain (PROT), and ATPase domain (AAA), in *E. coli*. Immunoblot against His-tagged (SLIMP) and FLAG-tagged (LON) from non-induced (NI), induced (I), input (IN), last wash (W), and elution (E).

(E) Quantification of mtDNA copy number normalized to control cells. The means of three independent experiments ± SDs are represented (*$p < 0.05$).

(F and G) Northern blot analysis (F) and quantification (G) of steady-state levels of mitochondrial mRNAs in SLIMP-, DmSerRS2-, or LON-depleted cells. The means of two independent experiments ± SDs normalized to Rp49 RNA levels are shown.

reflected in a drastic reduction in mitochondrial respiration activity (Figure S2D), but it does not immediately compromise organelle integrity, as evaluated by the levels of mitochondrial reactive oxygen species (ROS) (Figure S2E).

To characterize the SLIMP-DmSerRS2 interaction, we expressed affinity-tagged versions of both proteins in *Escherichia coli*. When expressed alone, DmSerRS2 is homodimeric, whereas SLIMP forms monomers and homodimers. When co-expressed, both proteins co-purified independently of the affinity tag used, confirming that SLIMP and DmSerRS2 form a tight complex (Figure 2C). Analysis of this complex by size exclusion chromatography and multiangle light scattering (MALS) unequivocally showed that DmSerRS2 and SLIMP form an αB heterodimer in solution (Figures 2D, S2F, and S2G). Our results show that SLIMP and DmSerRS2 are subunits of a heterodimeric mitochondrial SerRS required for $tRNA^{Ser}$ serylation and mitochondrial translation.

SLIMP Activates the Specific Degradation of TFAM by LON

LON is a broad-specificity mitochondrial protease that degrades the DNA-binding protein TFAM in *Drosophila*, thus repressing mtDNA levels (Matsushima et al., 2010). To study the functional connection between SLIMP and LON, we analyzed the impact of SLIMP depletion upon the degradation of TFAM. TFAM levels were increased 2-fold in cells depleted for SLIMP (Figure 3A), an effect that could be eliminated by overexpressing LON but not an inactive mutant of the protease (Figure 3B). We then used a synthetic peptide to monitor LON protease activity (Fishovitz et al., 2011) and found it to be independent of SLIMP, suggesting that SLIMP specifically stimulates the degradation of TFAM by LON through its interaction with the substrate-binding domain of the protease (Figure 3C).

To study the mechanism that drives the stimulation of TFAM degradation, we co-expressed affinity-tagged versions of SLIMP together with LON or the three structural domains of LON in *E. coli* (Venkatesh et al., 2012). Full-length LON and the isolated substrate-binding domain of LON readily co-purified with SLIMP (Figure 3D), suggesting that SLIMP modulates LON specificity through interactions with the substrate-binding domain of the protease.

SLIMP depletion *in vivo* led to an increase in mtDNA levels equivalent to the effect of LON depletion (Guitart et al., 2010), which is consistent with SLIMP's stimulating the degradation of TFAM by LON (Figure 3E). SLIMP depletion did not affect mitochondrial tRNA abundance (Figure S3A), but did cause a significant decrease in specific transcripts (Figures 3F and 3G). These results suggest that, overall, mtDNA transcription does not require SLIMP, but its depletion influences the stability or turnover rates of certain transcripts.

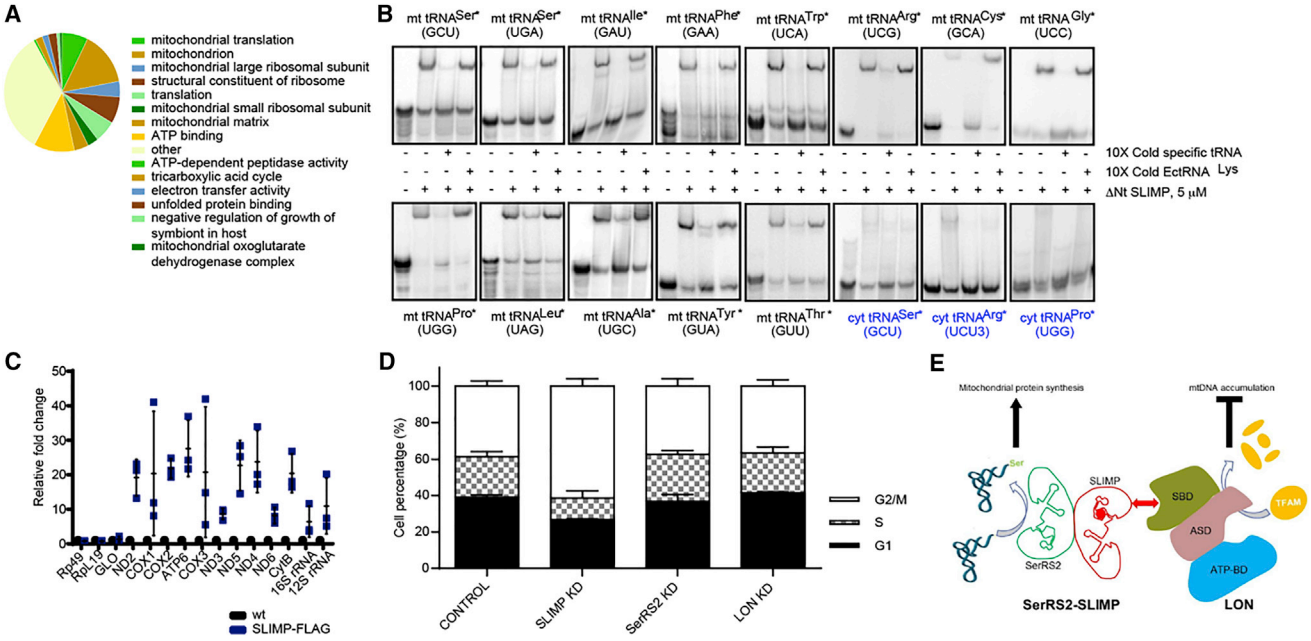

Figure 4. SLIMP Localizes Near Mitochondrial Ribosome Granules and Is Required for Cell-Cycle Progression

(A) Graphical representation of the subcellular localization of proximity interactors in SLIMP–BirA* or BirA* expressing cells.

(B) EMSA assays with radiolabeled mitochondrial (black) and cytosolic (blue) tRNAs and ΔN-SLIMP.

(C) Fold enrichment of target RNA sequences after immunoprecipitation of SLIMP-FLAG. The means of three independent experiments ± SDs are represented.

(D) Flow cytometry analysis of cell-cycle phase populations in control, SLIMP knockdown, DmSerRS2 knockdown, and LON knockdown cells. Data indicate means ± SDs of three independent experiments.

(E) Schematic representation of the interactions and functional roles of SLIMP in mitochondria.

See also Figures S3 and S4.

SLIMP Localizes near the Mitochondrial Ribosome Granules

As previously reported *in vivo*, SLIMP was predominantly found in the mitochondria (Figures S3B–S3E), a result confirmed by cell fractionation studies (Figure S3F). We determined the exact sequence of the mitochondrial targeting peptide that is cleaved upon mitochondrial import (Figure S3G). We then used BioID-mass spectrometry (BioID-MS) (Roux et al., 2013) to identify proteins localized to the vicinity of SLIMP (Figures S3H and S3I; Table S4). This analysis primarily revealed mitochondrial proteins involved in transcription and translation, including DmSerRS2 and LON (Figure 4A).

We asked whether SLIMP alone was capable of binding tRNAs or other nucleic acids. Electrophoretic mobility shift assays (EMSAs) showed that SLIMP binds most mitochondrial tRNAs with similar affinities (Figure 4B). Mitochondrial $tRNA^{Ser}_{(GCU)}$ and $tRNA^{Ser}_{(UGA)}$ transcripts were bound with dissociation constants of 1.79 and 1.677 μM, respectively (Figures S4A and S4B). Binding experiments with chimeric tRNAs, mitochondrial transcripts, and DNA showed that isolated SLIMP preferentially binds RNA structures with low folding energy in a sequence-independent manner (Figures 4C and S4C–S4G). Thus, SLIMP is unlikely to contribute to the tRNA specificity of SerRS2, and the fact that its depletion did not cause appreciable changes in mitochondrial tRNA levels indicates that SLIMP does not act as a tRNA chaperone (Figure S3A). However, the general affinity of SLIMP for RNA may explain its preferred localization in the vicinity of mitochondrial ribosome granules, which is consistent with its role in $tRNA^{Ser}$ aminoacylation as part of an SerRS2 heterodimer.

SLIMP Is Required for Cell-Cycle Progression

As SLIMP has previously been implicated in cell-cycle progression, we examined cell-cycle progression in *Drosophila* S2 cells following SLIMP depletion. Fluorescence-activated cell sorting (FACS) analysis revealed an increased percentage of cells in G2 phase upon SLIMP depletion (Figure 4D). This effect was not observed following the depletion of DmSerRS2 or LON (Figure 4D), indicating that the cell-cycle phenotype is specific to SLIMP depletion and suggesting that SLIMP may play additional roles in the control of cell-cycle progression.

DISCUSSION

The generation of mitochondrial biomass depends upon genes encoded in both the nucleus and the mitochondria, the translation of which must be coordinated to prevent an imbalanced composition of the mitochondrial proteome (Couvillion et al., 2016). At the same time, RNA transcription and DNA replication are potentially exclusive processes, the mutual interference of which must be prevented (Agaronyan et al., 2015). Thus, mechanisms must exist to control mitochondrial DNA levels and

transcription according to the translational needs of mitochondria and cell cycle.

It is well recognized that eukaryotic ARSs are a hotspot for the evolution of new functionalities, perhaps due to their ancient nature and multi-domain structures. SLIMP is an ARS paralog that evolved via the duplication of a mitochondrial SerRS gene early in the evolution of metazoans and was fixed in the genomes of arthropods. Our data indicate that SLIMP forms a heterodimer with a catalytically active SerRS2 monomer to generate a new form of mitochondrial SerRS2. SLIMP is essential for mitochondrial protein synthesis through its interaction with DmSerRS2, but the non-specific affinity of isolated SLIMP for unstructured RNAs suggests that SLIMP does not contribute to the substrate specificity of DmSerRS2. Nevertheless, the presence of SLIMP is essential for both tRNA aminoacylation and overall protein synthesis because the impact of its depletion in this regard is indistinguishable from the effect of depleting DmSerRS2. Although the analysis of the role of SLIMP in aminoacylation is complex due to the mutual dependence of SLIMP and SerRS2 for stability, our structural analysis of the SLIMP-SerRS2 complex by MALS and the lack of activity of the individually purified proteins support the existence of a stable SLIMP-SerRS2 heterodimer *in vivo*. These results beg the question of the selective advantage conferred upon arthropod cells by the duplication of the SerRS2-coding gene and the subsequent evolution of SLIMP. It is likely that SLIMP carries out non-canonical functions unrelated to translation, which may be coordinated and regulated through variations in the levels of SerRS2.

SLIMP also interacts with the substrate-binding domain of LON protease to stimulate the degradation of TFAM and prevent the accumulation of mtDNA. SLIMP depletion also affects the levels of specific mitochondrial transcripts, an observation that is consistent with the role of TFAM in the control of mitochondrial transcription (Falkenberg et al., 2002) (Figures 3F and 3G). The cellular localization of SLIMP, together with the fact that the SLIMP-LON interaction does not generally activate LON, suggests that SLIMP could recruit LON to stimulate TFAM degradation. Moreover, the fact that SLIMP interacts with the substrate-binding domain of LON opens the possibility that SLIMP actively contributes to the recognition of TFAM by LON.

We propose that SLIMP helps coordinate two intrinsically conflictive activities: mtDNA transcription and replication. SLIMP activity would repress mtDNA accumulation and stimulate the translation of transcripts. Under conditions in which mtDNA replication is preferential, attenuating SLIMP function would simultaneously reduce translation activity and increase mtDNA levels through TFAM accumulation.

Previous reports have highlighted the involvement of SLIMP in the control of cell-cycle progression in *Drosophila* (Ambrus et al., 2009; Liang et al., 2014). Our results confirm and extend these observations. We find that the involvement of SLIMP in the regulation of cell-cycle progression is likely independent of its interactions with SerRS2 and LON. This work, together with other reports showing that cytosolic SerRS regulates vascular development in animals (Amsterdam et al., 2004; Herzog et al., 2009; Xu et al., 2012), highlight the facility with which the SerRS structure incorporates non-canonical regulatory functions in animals. We propose that SLIMP evolved in arthropods as a mechanism to regulate translation and replication in mitochondria. It is possible that the coordination role of SLIMP extends to link mitochondrial physiological status with cell-cycle progression. Many evolutionary and mechanistic aspects of this regulatory network remain unknown, including whether functional equivalents to SLIMP exist in mammals.

STAR★METHODS

Detailed methods are provided in the online version of this paper and include the following:

- KEY RESOURCES TABLE
- CONTACT FOR REAGENT AND RESOURCE SHARING
- EXPERIMENTAL MODEL AND SUBJECT DETAILS
  - Cell Lines
- METHOD DETAILS
  - Immunoprecipitation
  - Immunoblotting
  - Pull-down Assay
  - Protein Cloning and Purification
  - SEC-MALLS Measurements
  - Aminoacylation Assays
  - *In Vivo* Labeling of Mitochondrial Translation Products
  - Electrophoretic Mobility Gel Shift Assay (EMSA)
  - Generation of Chimeric tRNAs
  - tRNA Folding Energy
  - Reverse Transcription and Quantitative Real-Time Polymerase Chain Reaction (qPCR)
  - BioID
  - Immunofluorescence
  - tRNA Northerns
  - Antibodies
  - LON Activity Assay
  - Flow-Cytometry-Based Assays for Mitochondrial ROS
  - Flow-Cytometry-Based Assays for Cell Cycle Analysis
  - Cell Fragmentation and Mitochondrial Isolation
  - Seahorse
- QUANTIFICATION AND STATISTICAL ANALYSIS

SUPPLEMENTAL INFORMATION

Supplemental Information can be found online at https://doi.org/10.1016/j.celrep.2019.03.022.

ACKNOWLEDGMENTS

This work was supported by grants SVP2014-068398 and BIO2015-64572 from the Spanish Ministry of Economy and Competitiveness (to L.R.d.P.). This work used the platforms of the Grenoble Instruct Centre (ISBG; UMS 3518 CNRS-CEA-UJF-EMBL) with support from FRISBI (ANR-10-INSB-05-02) and GRAL (ANR-10-LABX-49-01) within the Grenoble Partnership for Structural Biology (PSB). We would like to thank J.P. Muñoz, J. Bernués, J. Silva, A. Nebreda, S. Ackerman, P. Fox, and P. Schimmel for helpful input and discussions, and to thank the Mass Spectrometry and Biostatistics IRB core facilities for support. We thank ICTS "NANBIOSIS" and Unit 3 of the Bioengineering, Biomaterials and Nanomedicne CIBER (CIBER-BBN) for the synthesis of peptide FRETN89-98Abu.

AUTHOR CONTRIBUTIONS

D.P. and A.A.-F. performed the majority of the experiments and analyzed the data. N.C. carried out the purification and aminoacylation assays. A.P.-P. performed the mitochondrial fragmentation and mitochondrial signal peptide characterization. M.R.-E. carried out the co-expression and purification of SLIMP/SerRS2. A.M. and A.A.-F. performed the LON activity assays. M.C.-J., M.N.G., P.S., and A.A.-F. carried out the LON/SLIMP co-expression and purification. A.S. performed the Gene Ontology (GO) analysis. C.S. carried out the MALS experiments. S.L.H. performed the TFAM regulation experiments. P.A.K. carried out the BioID cloning. E.M.N. analyzed the data and performed the folding energy calculations. M.S.-V., L.S.K., and T.H.S. directed the research and provided critical advice and technical expertise. A.A.-F. and L.R.d.P. wrote the manuscript, and L.R.d.P. analyzed the data and directed the research.

DECLARATION OF INTERESTS

The authors declare no competing interests.

Received: December 3, 2018
Revised: February 13, 2019
Accepted: March 6, 2019
Published: April 2, 2019

REFERENCES

Agaronyan, K., Morozov, Y.I., Anikin, M., and Temiakov, D. (2015). Mitochondrial biology. Replication-transcription switch in human mitochondria. Science *347*, 548–551.

Alam, T.I., Kanki, T., Muta, T., Ukaji, K., Abe, Y., Nakayama, H., Takio, K., Hamasaki, N., and Kang, D. (2003). Human mitochondrial DNA is packaged with TFAM. Nucleic Acids Res. *31*, 1640–1645.

Ambrus, A.M., Rasheva, V.I., Nicolay, B.N., and Frolov, M.V. (2009). Mosaic genetic screen for suppressors of the de2f1 mutant phenotype in Drosophila. Genetics *183*, 79–92.

Amsterdam, A., Nissen, R.M., Sun, Z., Swindell, E.C., Farrington, S., and Hopkins, N. (2004). Identification of 315 genes essential for early zebrafish development. Proc. Natl. Acad. Sci. USA *101*, 12792–12797.

Arif, A., Terenzi, F., Potdar, A.A., Jia, J., Sacks, J., China, A., Halawani, D., Vasu, K., Li, X., Brown, J.M., et al. (2017). EPRS is a critical mTORC1-S6K1 effector that influences adiposity in mice. Nature *542*, 357–361.

Bailey, D., Urena, L., Thorne, L., and Goodfellow, I. (2012). Identification of protein interacting partners using tandem affinity purification. J. Vis. Exp. (*60*), 3643.

Bezawork-Geleta, A., Brodie, E.J., Dougan, D.A., and Truscott, K.N. (2015). LON is the master protease that protects against protein aggregation in human mitochondria through direct degradation of misfolded proteins. Sci. Rep. *5*, 17397.

Bogenhagen, D.F. (2012). Mitochondrial DNA nucleoid structure. Biochim. Biophys. Acta *1819*, 914–920.

Bota, D.A., and Davies, K.J. (2002). Lon protease preferentially degrades oxidized mitochondrial aconitase by an ATP-stimulated mechanism. Nat. Cell Biol. *4*, 674–680.

Chimnaronk, S., Gravers Jeppesen, M., Suzuki, T., Nyborg, J., and Watanabe, K. (2005). Dual-mode recognition of noncanonical tRNAs(Ser) by seryl-tRNA synthetase in mammalian mitochondria. EMBO J. *24*, 3369–3379.

Couvillion, M.T., Soto, I.C., Shipkovenska, G., and Churchman, L.S. (2016). Synchronized mitochondrial and cytosolic translation programs. Nature *533*, 499–503.

Cusack, S., Berthet-Colominas, C., Härtlein, M., Nassar, N., and Leberman, R. (1990). A second class of synthetase structure revealed by X-ray analysis of Escherichia coli seryl-tRNA synthetase at 2.5 A. Nature *347*, 249–255.

Dong, J., Qiu, H., Garcia-Barrio, M., Anderson, J., and Hinnebusch, A.G. (2000). Uncharged tRNA activates GCN2 by displacing the protein kinase moiety from a bipartite tRNA-binding domain. Mol. Cell *6*, 269–279.

Efeyan, A., Comb, W.C., and Sabatini, D.M. (2015). Nutrient-sensing mechanisms and pathways. Nature *517*, 302–310.

Eriani, G., Delarue, M., Poch, O., Gangloff, J., and Moras, D. (1990). Partition of tRNA synthetases into two classes based on mutually exclusive sets of sequence motifs. Nature *347*, 203–206.

Falkenberg, M., Gaspari, M., Rantanen, A., Trifunovic, A., Larsson, N.G., and Gustafsson, C.M. (2002). Mitochondrial transcription factors B1 and B2 activate transcription of human mtDNA. Nat. Genet. *31*, 289–294.

Fishovitz, J., Li, M., Frase, H., Hudak, J., Craig, S., Ko, K., Berdis, A.J., Suzuki, C.K., and Lee, I. (2011). Active-site-directed chemical tools for profiling mitochondrial Lon protease. ACS Chem. Biol. *6*, 781–788.

Fukui, H., Hanaoka, R., and Kawahara, A. (2009). Noncanonical activity of seryl-tRNA synthetase is involved in vascular development. Circ. Res. *104*, 1253–1259.

Gangelhoff, T.A., Mungalachetty, P.S., Nix, J.C., and Churchill, M.E. (2009). Structural analysis and DNA binding of the HMG domains of the human mitochondrial transcription factor A. Nucleic Acids Res. *37*, 3153–3164.

González, A., and Hall, M.N. (2017). Nutrient sensing and TOR signaling in yeast and mammals. EMBO J. *36*, 397–408.

Guitart, T., Leon Bernardo, T., Sagalés, J., Stratmann, T., Bernués, J., and Ribas de Pouplana, L. (2010). New aminoacyl-tRNA synthetase-like protein in insecta with an essential mitochondrial function. J. Biol. Chem. *285*, 38157–38166.

Guitart, T., Picchioni, D., Piñeyro, D., and Ribas de Pouplana, L. (2013). Human mitochondrial disease-like symptoms caused by a reduced tRNA aminoacylation activity in flies. Nucleic Acids Res. *41*, 6595–6608.

Guo, M., and Schimmel, P. (2013). Essential nontranslational functions of tRNA synthetases. Nat. Chem. Biol. *9*, 145–153.

Herzog, W., Müller, K., Huisken, J., and Stainier, D.Y. (2009). Genetic evidence for a noncanonical function of seryl-tRNA synthetase in vascular development. Circ. Res. *104*, 1260–1266.

Ibba, M., and Soll, D. (2000). Aminoacyl-tRNA synthesis. Annu. Rev. Biochem. *69*, 617–650.

Liang, L., Haug, J.S., Seidel, C.W., and Gibson, M.C. (2014). Functional genomic analysis of the periodic transcriptome in the developing Drosophila wing. Dev. Cell *29*, 112–127.

Markham, N.R., and Zuker, M. (2008). UNAFold: software for nucleic acid folding and hybridization. Methods Mol. Biol. *453*, 3–31.

Matsushima, Y., Goto, Y., and Kaguni, L.S. (2010). Mitochondrial Lon protease regulates mitochondrial DNA copy number and transcription by selective degradation of mitochondrial transcription factor A (TFAM). Proc. Natl. Acad. Sci. USA *107*, 18410–18415.

Meng, H., Yamashita, C., Hattori, N., and Imai, Y. (2017). Measurements of the mitochondrial respiration and glycolytic activity in Drosophila embryonic cells. Protocol Exchange, Published online July 10, 2017. https://doi.org/10.1038/protex.2017.069.

Park, S.C., Jia, B., Yang, J.K., Van, D.L., Shao, Y.G., Han, S.W., Jeon, Y.J., Chung, C.H., and Cheong, G.W. (2006). Oligomeric structure of the ATP-dependent protease La (Lon) of Escherichia coli. Mol. Cells *21*, 129–134.

Pinti, M., Gibellini, L., Liu, Y., Xu, S., Lu, B., and Cossarizza, A. (2015). Mitochondrial Lon protease at the crossroads of oxidative stress, ageing and cancer. Cell. Mol. Life Sci. *72*, 4807–4824.

Pinti, M., Gibellini, L., Nasi, M., De Biasi, S., Bortolotti, C.A., Iannone, A., and Cossarizza, A. (2016). Emerging role of Lon protease as a master regulator of mitochondrial functions. Biochim. Biophys. Acta *1857*, 1300–1306.

Ribas de Pouplana, L., and Schimmel, P. (2001). Two classes of tRNA synthetases suggested by sterically compatible dockings on tRNA acceptor stem. Cell *104*, 191–193.

Roux, K.J., Kim, D.I., and Burke, B. (2013). BioID: a screen for protein-protein interactions. Curr. Protoc. Protein Sci. *74*, Unit 19.23.

Saint-Léger, A., Bello, C., Dans, P.D., Torres, A.G., Novoa, E.M., Camacho, N., Orozco, M., Kondrashov, F.A., and Ribas de Pouplana, L. (2016). Saturation of recognition elements blocks evolution of new tRNA identities. Sci. Adv. *2*, e1501860.

Stahlberg, H., Kutejová, E., Suda, K., Wolpensinger, B., Lustig, A., Schatz, G., Engel, A., and Suzuki, C.K. (1999). Mitochondrial Lon of Saccharomyces cerevisiae is a ring-shaped protease with seven flexible subunits. Proc. Natl. Acad. Sci. USA *96*, 6787–6790.

Teo, G., Liu, G., Zhang, J., Nesvizhskii, A.I., Gingras, A.C., and Choi, H. (2014). SAINTexpress: improvements and additional features in Significance Analysis of INTeractome software. J. Proteomics *100*, 37–43.

Venkatesh, S., Lee, J., Singh, K., Lee, I., and Suzuki, C.K. (2012). Multitasking in the mitochondrion by the ATP-dependent Lon protease. Biochim. Biophys. Acta *1823*, 56–66.

Villa-Cuesta, E., and Rand, D.M. (2015). Preparation of Mitochondrial Enriched Fractions for Metabolic Analysis in Drosophila. J. Vis. Exp. Published online September 30, 2015. https://doi.org/10.3791/53149.

Xu, X., Shi, Y., Zhang, H.M., Swindell, E.C., Marshall, A.G., Guo, M., Kishi, S., and Yang, X.L. (2012). Unique domain appended to vertebrate tRNA synthetase is essential for vascular development. Nat. Commun. *3*, 681.

Yao, P., Poruri, K., Martinis, S.A., and Fox, P.L. (2014). Non-catalytic regulation of gene expression by aminoacyl-tRNA synthetases. Top. Curr. Chem. *344*, 167–187.

STAR★METHODS

KEY RESOURCES TABLE

REAGENT or RESOURCE	SOURCE	IDENTIFIER
Antibodies		
Anti-DmSLIMP	Guitart et al., 2010	N/A
Anti-DmLON	Matsushima et al., 2010	N/A
Anti-DmSerRS2	Guitart et al., 2013	N/A
Anti-DmSerRS1	Guitart et al., 2013	N/A
Anti-FLAG	Sigma-Aldrich	Cat. #F3165; RRID:AB_259529
Anti-betaATPase	Guitart et al., 2010	N/A
Anti-betaTubulin	Hybridoma Bank	Cat. #E7; RRID:AB_528499
Anti-VDAC/porin	Abcam	Cat. #ab14734; RRID:AB_443084
Anti-TFAM	Matsushima et al., 2010	N/A
Anti-His	Abcam	Cat.#ab18184; RRID:AB_444306
Chicken HRP	Chemicon International	Cat. #AP194P; RRID:AB_92682
Mouse HRP	Amersham	Cat. #NA931; RRID:AB_772210
Rabbit HRP	Amersham	Cat. #NA934; RRID:AB_772206
Mouse Alexa 488	Invitrogen	Cat. #A21202; RRID:AB_141607
Rabbit Alexa 488	Invitrogen	Cat. #A11008; RRID:AB_143165
Bacterial and Virus Strains		
Expression strain BL21	NzyTech	Cat. #MB006
Cloning strain DH5alpha	Bionova	Cat. #60602-2
Chemicals, Peptides, and Recombinant Proteins		
FRETN89-98Abu	Fishovitz et al., 2011	N/A
EasyTag L-35S-methionine	Perkin Elmer	NEG709A005MC
Critical Commercial Assays		
Pierce BCA Protein Assay Kit	Thermo	Cat. #23225
ECL Select Western Blotting Detection Reagent	GE Healthcare	Cat. #RPN2235
HisTrap HP histidine-tagged	GE Healthcare	Cat. #17524701
Anti-FLAG® M2 Magnetic Beads	Sigma	Cat. # M8823
SYBR Green PCR Master Mix	Thermo	Cat. # 4309155
MitoSox	Molecular probes	Cat. #M36008
Seahorse	Agilent	Cat. #103015-100
IgG Sepharose 6 Beads	GE Healthcare	Cat. #17096901
Dynabeads M-280 Streptavidin	Thermo	Cat. #11205D
Experimental Models: Cell Lines		
D. melanogaster: Cell line S2: S2-DRSC	Azorin's lab (IRB Barcelona)	FlyBase: FBtc0000181
Primers list - see Table S5		
Recombinant DNA		
pMK33 vector	This paper	N/A
pET-duet vector	This paper	N/A
pQE-70 vector	Guitart et al., 2010	N/A
Other		
Schneider's *Drosophila* media	Lonza	Cat. #04-351Q
Fetal Bovine Serum	GIBCO	***Cat. # 10270106***
Effectene	***QIAGEN***	***Cat. # 301425***

CONTACT FOR REAGENT AND RESOURCE SHARING

Further information and requests for resources and reagents should be directed to and will be fulfilled by the lead contact, Lluís Ribas de Pouplana: lluis.ribas@irbbarcelona.org.

EXPERIMENTAL MODEL AND SUBJECT DETAILS

Cell Lines

Drosophila Schneider 2 cells (S2) (male) were maintained at 25°C on Schneider's *Drosophila* medium (Lonza) supplemented with 10% fetal bovine serum (FBS) and 50 μg/ml penicillin and streptomycin. S2 cells were transfected using Effectene (QIAGEN) and stable cell cultures were selected by adding 200 μg/ml hygromycin B (GIBCO) to the media. All silencing experiments reported were carried out after an eight-day induction initiated by the addition of 400μm $CuSO_4$ to the media.

METHOD DETAILS

Immunoprecipitation

Drosophila melanogaster S2 cells overexpressing SLIMP-FLAG, DmSerRS2-FLAG or S2 wild-type were used for each immunoprecipitation (IP) or Co-IP reaction. Total cellular proteins were extracted in 100 μl IP lysis buffer (50 mM Tris HCl pH 8, 150 mM NaCl, 1% NP-40, 0.5% sodium deoxycholate, 0.1% SDS), or 100 μl Co-IP buffer (20 mM Tris HCl pH 8, 137 mM NaCl, 1% Nonidet P-40 (NP-40), 2 mM EDTA), in the presence of complete protease inhibitors (Roche), and lysed on ice for 45 min on a rotating wheel. Cellular extracts were centrifuged at 25,000 g at 4°C, for 30 min and supernatants were mixed with proper antibody-conjugated beads for immunoprecipitation. Samples from cells overexpressing SLIMP-FLAG and DmSerRS2-FLAG samples were immunoprecipitated with anti-FLAGM2-conjugated magnetic Dynabeads (Invitrogen), or with an antibody against LON cross-linked to protein-A Sepharose beads overnight at 4°C in orbital rotation. Immunoprecipitation was performed with Dynabeads protein A (Invitrogen) following manufacturer's instructions, except for the incubation of the antibody with the beads, and the incubation of the extract with antibody cross-linked to the beads, which were both carried out overnight. The IP or Co-IP fractions were finally analyzed by immunoblotting. For treatment with nucleases, 100 μg/ml of RNase A (Sigma) and 2U of MNase (Fermentas) were added, and the mixture was incubated for 10 min at 37°C.

Immunoblotting

Protein lysates were quantified by Pierce BCA Protein Assay Kit (Thermo Fisher Scientific), and equal protein amounts were resolved on polyacrylamide gels in Tris-glycine running buffer. Gels were transferred to polyvivylidene fluoride (PVDF) membranes (Immobilon-P, Millipore). Membranes were blocked with 5% milk TBS-T for one hour, and incubated with the appropriate dilution of the primary and secondary antibodies. Antibody detection was done by using ECL chemiluminescent system (Amersham), and exposure to X-ray film (Fujifilm) or using the Odyssey Infrared Imaging System (Li-Cor; Lincoln, NE).

Pull-down Assay

Pull-down of SLIMP protein partners was performed according to published protocols with several modifications (Bailey et al., 2012). First, a *Drosophila melanogaster* S2 cell line overexpressing SLIMP-TAP tagged was created. We performed the pull-down procedure with only one affinity tag (one step TAP purification) via Protein A-IgG interaction. Cells expressing SLIMP were collected, washed twice with ice-cold PBS, and lysed in TAP lysis buffer A (0,46M sacarose, 120mM KCl; 30mM NaCl, 0,5mM MgCl2, 1mM spermine, 0,3mM spermidine, 30mM Tris pH 7.4, 28mM beta-mercaptoethanol, 1x complete protease inhibitor by Roche) through 50 strokes with a loose pestle in ice. Debris were collected by centrifugation, and supernatant was lysed again in TAP lysis buffer B (40mM HEPES-KOH pH 7.9, 40% glycerol, 0,6M NaCl, 3mM MgCl2, 1mM EGTA, 1mM DTT, 1x complete protease inhibitor by Roche) and further 50 strokes with a tight pestle on ice. 0,1% NP-40 was added to the cellular lysate, and samples were incubated for 20 min at 4°C on a rotating wheel. Cell debris were centrifuged, and an aliquot of supernatant was saved as "Input." The rest of the lysate was mixed with previously washed IgG Sepharose Fast 6 flow (GE Healthcare) beads, and incubated overnight at 4°C using a rotating wheel. After binding, Sepharose beads were collected by centrifugation, washed 4 times in chilled lysis buffer and washed 3 more times in wash buffer (20mM HEPES pH 7.9, 20% glycerol, 0,3M NaCl, 0,1% NP-40, 0,5mM EGTA, 0,5mM DTT, 1x complete protease inhibitors). After the final wash the remaining buffer was removed, and the tagged protein was eluted from the streptavidin beads by adding 50mM Glycine-HCl pH 3 and incubating at room temperature for 5 minutes. Beads were then collected by centrifugation, supernatant containing the tagged protein and interacting proteins was supplemented with SDS protein loading buffer, boiled, and stored for further analysis. Eluted samples were analyzed by SDS-PAGE, Colloidal Coomassie staining and, mass spectrometry for protein identification.

Protein Cloning and Purification

SLIMP, DmSerRS2 and SRS1 were cloned into the pQE-70 vector (QIAGEN) for bacterial expression of a C-terminal 6His-tagged protein. The sequence of the plasmid was confirmed by sequencing. SLIMP and DmSerRS2 were cloned into pOPINFS expression

vectors (Oxford Protein Production Facility) as a bicistronic product, resulting in a C-terminal 6His-taggged DmSerRS2 and C-terminal Strep II tagged SLIMP separated by a ribosome binding site. BL21 (DE3) cells (Nzythech) were transformed. The starter culture was diluted 1/100 in autoinduction media at 37°C for 2 hours, and 17 hours at 25°C until the OD600 was stable. Cell pellet was resuspended in lysis buffer (20mM sodium phosphate buffer, 200mM NaCl, 50 mM imidazole, protease inhibitor cocktail, and DNaseI) and lysed using a cell disruptor (20kPsi). The lysate was centrifuged at 24000 g for 1 hour, and the supernatant was filtered with a 0.45 μm filter. The enzymes were purified on HisTrap columns according to manufacturer's protocol (GE Healthcare Life Sciences). The collected fractions were analyzed by SDS-PAGE and dialyzed (20mM sodium phosphate buffer, 200mM NaCl, 1mM DTT). Proteins were stored in dialysis buffer with 10% glycerol, and protein concentration was measured with Pierce BCA Protein Assay Kit (Thermo Fisher).

SLIMP C-terminal His and LON C-terminal Flag tagged or its separate domains, and SerRS2 and LON C-terminal Flag tagged, were cloned into pET-duet expression vectors as a bicistronic product. BL21 (DE3) cells (Nzythech) were transformed. The starter culture was diluted 1/100 in LB media at 37°C for 2 hours, and 2.5h hours at 37°C in 1mM IPTG. Cell pellet was resuspended in lysis buffer (PBS, protease inhibitor cocktail, and DNaseI) and lysed using cell sonication (15 s on 15 s off for 5 min at 3%). The lysate was centrifuged at 24000 g for 1 hour. The enzymes were purified using anti-FLAGM2-conjugated magnetic Dynabeads (Invitrogen) according to manufacturer's protocol. The elution was analyzed by SDS-PAGE and western blot.

SEC-MALLS Measurements

50 μL of NiNTA purified samples were filtered with 0.1 μm (Ultafree, Millipore), and injected at concentrations of 1 mg/mL (DmSerRS2), 2.6 mg/mL (SLIMP) and 3.1 mg/mL (DmSerRS2/SLIMP-complex) into a Superdex 200_10/300 (GE Healthcare) column equilibrated in 20 mM Sodium phosphate pH 7.4, 200 mM NaCl, 1 mM DTT buffer at room temperature and a flow rate of 0.5 mL/min. The column was coupled to a MALLS system that included a DAWN-HELEOS-II detector (Wyatt Technology) with a laser emitting at a wavelength of 664.3 nm. Concentrations were measured with an Optilab T-rEX differential refractive index detector (Wyatt Technology) with a differential index of refraction (dn/dc) of 0.185 mL/g. Molecular weights were calculated using ASTRA software (Version 6.0.5.3, Wyatt Technology), and averaged over the main peaks of elution.

Aminoacylation Assays

tRNAs were obtained by *in vitro* transcription using T7 RNA polymerase according to standard protocols(Saint-Léger et al., 2016). *In vitro* tRNA aminoacylation assays were performed at 25°C in 100 mM HEPES pH 7.2, 40 mM KCl, 50 mM MgCl2, 1 mM ATP, 0.1 mg/ml − 1 BSA, 1 mM DTT, 10 μM serine, 500 Ci/mol − L–[3H (G)]-Serine and 0.5 μM protein. Reaction was initiated by addition of pure enzyme and samples of 22 μL were spotted onto Whatman 3 MM discs at varying time intervals. Radioactivity (corresponding to amino acid ligated to tRNA substrate) was measured by liquid scintillation (TriCard 2900TR, Packard).

In Vivo Labeling of Mitochondrial Translation Products

Cells were harvested at room temperature, and washed twice with methionine-free Grace's insect medium (GIBCO) supplemented with 10% FBS, 200μg/ml emetine, and 100 μg/ml cycloheximide. Five minutes after cell resuspension, EasyTag L-35S-methionine (Perkin Elmer, NEG709A005MC) was added to a final concentration of 200uCi/ml, and the cells were incubated for 3h at 25°C. After incubation, the cells were diluted with 2 volumes of Schneider Medium, and washed twice with PBS. The cells were lysed in RIPA buffer. Total cellular protein (50 μg per lane) was separated by SDS-PAGE. Gels were transferred to polyvivylidene fluoride (PVDF) membranes (Immobilon-P, Millipore) at 250 mA for 90 minutes at 4°C in transfer buffer. The membrane was dried 30 minutes at room temperature, exposed to a Storage Phosphor Screen (Molecular Dynamics) for 15 days, and imaged using a Typhoon 8600 Variable Mode Imager (Molecular Dynamics).

Electrophoretic Mobility Gel Shift Assay (EMSA)

Drosophila melanogaster tRNAs and mRNAs were *in vitro* transcribed using T7 RNA polymerase following standard methods, labeled with γ-[32P]-ATP using T4 polynucleotide kinase, refolded by incubation at 90°C, slow cooled to room temperature, and incubated for 20 minutes at 4°C in 30 mM MgCl2, 30 mM KCl, 1 mM dithiothreitol (DTT), 20% (w/v) glycerol, 150 mM Tris buffer pH 7.0, 40 ng/μl oligo(dT)25 with ΔNt-SLIMP recombinant protein. For double strand oligonucleotides EMSA, 10μl of HPLC purified synthetic oligonucleotides (Sigma) were labeled with γ-[32P]-ATP using T4 polynucleotide kinase, purified through a G50 Sephadex column, and annealed with the complementary oligonucleotides o/n in 10 mM Tris, pH 7.5–8.0, 50 mM NaCl, 1 mM EDTA by incubation at 85°C and slow cooling to room temperature. The hybridized mixture was diluted at 50nM final concentration in binding buffer (20mM HEPES pH 8, 150mM KCl, 125uM EDTA, 1mM DTT, 0.626 mg/ml BSA) with ΔNt-SLIMP or Human TFAM recombinant proteins. Each binding reaction was separated by electrophoresis onto a 6% (w/v) polyacrylamide gel in TBE 0.5X. Gels were dried at 80°C for 1h and signals were digitalized from dried gels exposed in a storage phosphor screen.

Generation of Chimeric tRNAs

The plasmids created for the *in vitro* transcription of *D. melanogaster* $tRNA^{Ser}$ (GCU) chimeras are derived from the ligation of a synthetic DNA sequence between the HindIII and BamHI sites of the *E. coli* plasmid pUC19. The inserted sequence contains a T7 RNAP promoter followed by the desired tRNA gene which contains a BstNI site immediately after the tRNA gene. The plasmid is used, after

digestion with BstNI, as a template for an *in vitro* transcription reaction for the production of tRNA molecules. Exchanges of nucleotides between mitochondrial and cytosolic $tRNA^{Ser}$ sequences are underlined. Chimeras 1-5 are made of the mitochondrial $tRNA^{Ser}$ backbone with substitutions of some nucleotides from the cytosolic $tRNA^{Ser}$ sequence. Chimeras 6-10 are made of cytosolic $tRNA^{Ser}$ backbone with nucleotide substitutions from the mitochondrial $tRNA^{Ser}$ sequence.

tRNA Folding Energy

The folding energies of all *in vitro* transcribed RNAs used in our assays were computed using UNAFold(Markham and Zuker, 2008) version 3.8.

Reverse Transcription and Quantitative Real-Time Polymerase Chain Reaction (qPCR)

Total RNA was extracted from cultured cells with TRIzol (Invitrogen) or with RNeasy MinElute (QIAGEN), digested with DNase I and cleaned with the RNeasy Cleanup kit (QIAGEN). 500 ng of total RNA was retrotranscribed into cDNA using random primers (Reverse Transcription System, Promega-A3500) to perform quantitative real-time polymerase chain reactions (RT-qPCR) by means of Power SYBR Green and a StepOnePlus Real-time PCR System (Applied Biosystems) following manufacturer's instructions. Total DNA was extracted with TRIzol (Invitrogen) and mtDNA was also quantified by real-time qPCR. Genomic DNA templates from S2 cells were amplified with primers designed to amplify the mitochondrial gene ATPase6, and the gene mRp110 used as a control for nuclear gene.

BioID

Stable S2 cell lines with BirA or SLIMP-BirA vector were produced. Stable cell lines were seeded ± 50 μM biotin (Panreac 143977), and 400 μM CuSO4 during 24h. Cells were collected by and washed 2X in PBS before lysate them in modified RIPA buffer (150mM Tris-HCl pH 7.5, 150mM NaCl, 1mM EDTA, 1mM EGTA, 1% Triton X-100, 0.1% SDS, protease inhibitor cocktail (Roche)) on ice.

Biotinylated proteins were isolated using streptavidin Dynabeads M-280 (Invitrogen), washed 3X in PBS and digested with trypsin and analyzed by mass spectrometry.

For the quantitative analysis, contaminant identifications were removed and unique peptide spectrum matches of protein groups identified with Sequest HT were analyzed with SAINTexpress-spc v3.1(Teo et al., 2014). Control samples (BirA) were compared to SLIMPBirA samples. High confidence interactors were defined with a SAINT score $\geq$ 0.7.

For the Gene Ontology analysis proteins with a fold change $\geq$ 1.5 were selected. A proportion test was used to compare the number of times each GO term in the list and the number of times each GO term appears in the whole proteome with a p value $<$ 0.01.

Immunofluorescence

For Immunofluorescence studies, coverslips were pre-treated with 500 μg concanavalin A (Sigma) for 20 min, aspirated and allowed to dry. Following a 1 mL rinse with complete Schneider media, 500 μL of S2 cells were added to 1.5ml of complete Schneider media and incubated for 1h on treated coverslips. Culture media was aspirated from each well and coverslips were rinsed gently three times in PBS. Cells were fixed to coverslips in 4% paraformaldehyde (in PBS) for 10 min and rinsed three times in PBS. Cells were permeabilized with IF buffer (0,1% Triton X-100 and 0,1% BSA in PBS) during 20 min and incubated with primary antibodies at concentration 1:500 in IF solution overnight at 4°C. Cells are then washed 3X with IF buffer, and incubated with fluorophore-conjugated secondary antibodies in IF buffer for 1 h at room temperature protected from light. Cells are then washed twice with IF wash solution (0,1% Triton X-100 in PBS) and 2x in PBS. Cells were stained with DAPI (Sigma) in PBS for 5 minutes in the dark and then washed 3X in PBS. Coverslips were drained and mounted on slides with the fluorescent preservative Mowiol 4-88 (Merck). Images were acquired by using a Leica SP5 confocal laser-scanning microscope. Image processing was done using Fiji software. For mitochondria labeling, S2 cells are incubated with 100nM MitoTracker Red CMXRos (Invitrogen-M7512) for 15 min prior fixation.

tRNA Northerns

Mini gels were tRNA are separated are transferred to nylon membrane (Hybond XL, Amersham) in TAE at 500 mA for 2 h at 4°C using in the Mini Trans-Blot cell. After transfer is complete, tRNAs are UV cross-linked to membrane with using Stratalinker UV Crosslinker 1800 (Stratagene). Synthetic oligonucleotides labeled with [γ32P]ATP (PerkinElmer-NEG002A250UC, 3000 Ci/mmol) on the 5′ end are used as probes. Oligonucleotides are kinased by incubating the 20 μL reaction mix (10 pmol of oligonucleotide, 1x kinase buffer, 0.75 U/μl T4PNK, 10 mM spermidine, 750 Ci/mol [γ32P]ATP) for 1h at 37°C. Phosphorylation reactions are then extracted with PCIA 25:24:1 pH 6.7/8.0. The labeled probes can be stored at -20°C and used within 2 weeks. Dried membranes are soaked in 0.2x SSPE (10mM NH2PO4, 150 mM NaCl, 1mM EDTA pH 7.4) for few min, placed in the hybridization bottles and pre-hybridized at the 55°C with 20 mL of hybridization buffer (6x SSPE buffer, 10x Denhardt's, 0.5% w/v SDS) for 1h in the oven under rotation. Following the pre-hybridization, 33-100 μL of the labeled probe are added and allowed to hybridize for 16 hours. Unbound probe is removed by washing the membrane twice for 3 min with room temperature washing buffer and twice for 3 min with washing buffer (2x SSPE; 0.5% SDS) pre-warmed at the corresponding hybridization temperature, always in the oven under rotation. The washed membrane is then placed within plastic wrap, sealed, placed on the cassette, covered with the Hyperscreen and exposed for 16 hours. The signals are digitalized in the PhosphorImager through Typhoon Scanner Control software and quantified using Fiji software.

Antibodies

A polyclonal (rabbit) SLIMP antibody was isolated by Antibody BCN using full-length purified protein as antigen. Other antibodies used were α-LON (Dr. Kaguni, Michigan S. University), α-DmSerRS2 (Innovagen), α-DmSerRS1 (Innovagen), α-FLAG (Sigma), α-βATPase (Dr. Garesse, Instituto de Investigaciones Biomédicas – Universidad Autónoma de Madrid), α-βtubulin (Hybridoma Bank), α-VDAC/porin (Abcam), α-TFAM (Dr. Kaguni), α-His tag (Abcam), chicken HRP (Chemicon Int.), mouse HRP (Amersham), and rabbit HRP (Amersham), mouse and rabbit Alexa 488 (Invitrogen).

LON Activity Assay

S2 cells were collected and washed with PBS. Cell pellet was resuspend in ice-cold Cell Buffer (225 mM mannitol, 75 mM sucrose, 0.1 mM EGTA, 30 mM Tris-HCl, pH 7.4), and homogenized using a tight douncer (25 strokes). The homogenate was centrifuged at 300 g for 5 minutes at 4°C, the supernatant was collected in a new Eppendorf, and centrifuged at 6000 g for 10 minutes at 4°C. The mitochondrial pellet was washed twice in Wash Buffer (225 mM mannitol, 45 mM sucrose, 10 mM KCl, 10 mM Tris-HCl, 5 mM KH_2PO_4, pH 7.4), and the final pellet was resuspend in Reaction Buffer (50 mM HEPES pH 8, 5 mM $Mg(OAc)_2$, 2 mM DTT, 5 mM imidazole).

Monitoring of the specific activity of LON protease was performed as previously reported (Fishovitz et al., 2011). FRETN 89-98Abu was synthesized according to the published protocols (Fishovitz et al., 2011). Reactions were performed in black 96 well assay plates (Costar) in 200 μl reaction buffer, 1 mM ATP, 100 μM FRETN 89-98Abu, and 35 μg of isolated mitochondria. The fluorescent emission (420 nm) was monitored during 3 hours by Infinite plate reader (Tecan).

Flow-Cytometry-Based Assays for Mitochondrial ROS

To detect mitochondrial ROS production, cells were incubated at 25°C for 30 min in 5 μM MitoSox (Molecular Probes, M36008), washed once with PBS and immediately analyzed by flow cytometry. Data were collected with a Gallios flow cytometer using Kaluza for Gallios software (Beckman Coulter).

Flow-Cytometry-Based Assays for Cell Cycle Analysis

Cells were collected, washed with PBS and fixed in 70% ice-cold ethanol for at least 2 h. Cells were permeabilized with PBS containing 0.25% Triton X-100, and incubated at 37°C for 30 minutes in PBS containing 40 μg/ml RNase A and 1 μg/ml propidium iodide. Flow cytometric experiments were carried out using an Epics Cyan ADP flow cytometer (Beckman Coulter, Inc, U.S). The instrument was set up with the standard configuration. Excitation of the sample was done at 488nm. Forward scatter (FSC), side scatter (SSC) and red (613/20 nm) fluorescence for PI were recorded. PI fluorescence was projected on a mono-parametrical histogram. Aggregates were excluded gating single cells by their area versus peak fluorescence signal. Time was used as a control of the stability of the instrument. Histograms were analyzed using Multicycle Software (Phoenix).

Cell Fragmentation and Mitochondrial Isolation

Mitochondrial isolation was performed as previously reported (Villa-Cuesta and Rand, 2015).

Seahorse

Mitochondrial respiration was measured as previously reported (Meng et al., 2017) with minor modifications. S2 cells were grown and induced for eight days, counted and $2 \cdot 10^6$ cells/ml were plated in concanavalin A coated plates. MitoStress assay was performed according to the manufacturer's protocol.

QUANTIFICATION AND STATISTICAL ANALYSIS

Statistical analyses were performed with GraphPad Prism software version 6.0 (GraphPad Software). Data are shown as the mean ± S.E.M or mean ± SD, as indicated in each figure. A two-tailed t test was performed when comparing two groups with normal distribution. An ANOVA test followed by a Dunnett multiple comparison was used to compare more than two groups.